



A basin redox transect at the dawn of animal life



Erik A. Sperling^a, Galen P. Halverson^b, Andrew H. Knoll^a, Francis A. Macdonald^{a,*}, David T. Johnston^{a,**}

^a Department of Earth and Planetary Sciences, Harvard University, Cambridge, MA 02138, USA

^b Department of Earth and Planetary Sciences/GEOTOP, McGill University, Montreal, Quebec, Canada H3A 2A7

ARTICLE INFO

Article history:

Received 30 October 2012

Received in revised form

1 April 2013

Accepted 4 April 2013

Editor: G. Henderson

Available online 3 May 2013

Keywords:

Cryogenian
Fifteenmile Group
Canada
oxygen
animals
physiology

ABSTRACT

Multiple eukaryotic clades make their first appearance in the fossil record between ~810 and 715 Ma. Molecular clock studies suggest that the origin of animal multicellularity may have been part of this broader eukaryotic radiation. Animals require oxygen to fuel their metabolism, and low oxygen levels have been hypothesized to account for the temporal lag between metazoan origins and the Cambrian radiation of large, ecologically diverse animals. Here, paleoredox conditions were investigated in the Fifteenmile Group, Ogilvie Mountains, Yukon, Canada, which hosts an 811 Ma ash horizon and spans the temporal window that captures the inferred origin and early evolution of animals. Iron-based redox proxies, redox-sensitive trace elements, organic carbon percentages and pyrite sulfur isotopes were analyzed in seven stratigraphic sections along two parallel basin transects. These data suggest that for this basin, oxygenated shelf waters overlay generally anoxic deeper waters. The anoxic water column was dominantly ferruginous, but brief periods of euxinia likely occurred. These oscillations coincide with changes in total organic carbon, suggesting euxinia was primarily driven by increased organic carbon loading. Overall, these data are consistent with proposed quantitative constraints on Proterozoic atmospheric oxygen being greater than 1% of modern levels, but less than present levels. Comparing these oxygen levels against the likely oxygen requirements of the earliest animals, both theoretical considerations and the ecology of modern oxygen-deficient settings suggest that the inferred oxygen levels in the mixed layer would not have been prohibitive to the presence of sponges, eumetazoans or bilaterians. Thus the evolution of the earliest animals was probably not limited by the low absolute oxygen levels that may have characterized Neoproterozoic oceans, although these inferred levels would constrain animals to very small sizes and low metabolic rates.

© 2013 Elsevier B.V. All rights reserved.

1. Introduction

A number of eukaryotic groups first appear in the fossil record between the Bitter Springs isotope excursion at ~810 Ma and the Sturtian glaciation at ~715 Ma (Macdonald et al., 2010). This apparent radiation includes the first unequivocal appearances of groups such as the vase-shaped microfossils, interpreted to be related to lobose, and perhaps filose, testate amoebae (Porter and Knoll, 2000; Porter et al., 2003), scale microfossils of uncertain phylogenetic affinity (Cohen et al., 2011; Cohen and Knoll, 2012), and simple multicellular and coenocytic green algae (Butterfield et al., 1994). Interestingly, molecular clock studies suggest that the origin of animal multicellularity may have been part of this broader radiation. Studies utilizing different taxa, genes, calibration points and clock models have converged on an estimated divergence of ~800 Ma for the last common ancestor of animals

(Berney and Pawłowski, 2006; Lartillot et al., 2009; Sperling et al., 2010; Erwin et al., 2011; Parfrey et al., 2011). Similar results in these studies, despite broad methodological differences, suggest this divergence estimate is approximately correct. This age finds further support in the appearance of presumed demosponge-specific biomarkers beneath ca. 635 Ma Marinoan glacial deposits (Love et al., 2009; Kodner et al., 2008); as demosponges represent a derived lineage within animals, the origin of the animal crown group must be even deeper in time. If the molecular clock ages and biomarker data are accurate, the lack of metazoan body and trace fossils throughout the Cryogenian and early Ediacaran periods presents a conundrum (Erwin et al., 2011). It has been hypothesized that animal body size and diversity may have been limited by relatively low levels of oxygen in the Proterozoic atmosphere and oceans. In such oceans, it is posited that animals could have been restricted to small and thin body plans that did not fossilize well, with the explosion of larger and ecologically diverse organisms in the late Ediacaran and Cambrian related in part to increasing O₂ levels (Cloud, 1968; Rhoads and Morse, 1971; Runnegar, 1982a; Knoll and Carroll, 1999). Consistent with this hypothesis, different geochemical redox proxies support

* Corresponding author. Tel.: +1 617 496 2236; fax: +1 617 384 7396.

** Corresponding author. Tel.: +1 617 496 5024; fax: +1 617 384 7396.

E-mail addresses: fmacdon@fas.harvard.edu (F.A. Macdonald), johnston@eps.harvard.edu (D.T. Johnston).

a directional change toward more oxygenated conditions in the latest Proterozoic (reviewed by Och and Shields-Zhou (2012) and Kah and Bartley (2011)).

What remains highly uncertain, however, are the atmospheric and oceanic oxygen concentrations prior to and during earliest animal evolution, specifically during the Cryogenian period (850–635 Ma). Oxygen levels are generally assumed to have been relatively low in Cryogenian oceans (e.g. Kump, 2008), but given the lack of widespread paleoenvironmental documentation, the extent to which early animals were limited by low oxygen levels remains unknown. Specifically, the physiological requirements of small animals with low-energy lifestyles that may have characterized the Cryogenian period were likely different from the larger, more active and muscular organisms preserved in Cambrian rocks. This difference

needs to be considered when comparing physiological requirements against the constraints provided by geochemical proxies.

Here, we investigate the environmental context of early animal evolution and compare inferred redox constraints with the likely physiological requirements associated with different grades of organization in early animal evolution. Previous iron speciation and sulfur isotope studies of the pre-Sturtian Chuar Group (Canfield et al., 2008; Nagy et al., 2009; Johnston et al., 2010) provide insight into Cryogenian environments, but are limited to a single section deposited between ca. 770 and 742 Ma (Karlstrom et al., 2000). Here we report geochemical redox proxies through seven sections along two parallel platform-to-basin transects in the early Cryogenian Fifteenmile Group in the Tatonduk and Coal Creek inliers, Ogilvie Mountains, Yukon, Canada (Figs. 1 and 2). The Fifteenmile Group was deposited in a basin that originated during an episode of continental extension (Macdonald et al., 2012) prior to 811.51 ± 0.25 Ma, the U–Pb zircon date on a tuff in the upper portion of the Reefal Assemblage (green line in Mt. Harper Section, Figs. 3 and 6; Macdonald et al., 2010). Thus the Fifteenmile Group spans a time period that significantly preceded the earliest macroscopic multicellular forms in the Ediacaran period (Narbonne, 2011) but overlaps with molecular-clock estimates for the divergence of crown-group animals (Erwin et al., 2011, and references above).

The paleoredox state of shale samples collected from measured stratigraphic sections was investigated using a multi-proxy approach. Specifically, iron speciation data are integrated with major-element and redox-sensitive trace element abundances, total organic carbon (TOC) percentages, and pyrite sulfur isotope values to obtain an estimate of overall water-column redox profiles. Together, the geochemical data from these stratigraphic sections provide the first early Neoproterozoic basin redox transect and give insight into paleoenvironmental conditions in this basin at the dawn of animal life. These



Fig. 1. Location map of the Coal Creek and Tatonduk inliers, Yukon Territory, Canada, with stars marking the location of the inliers.

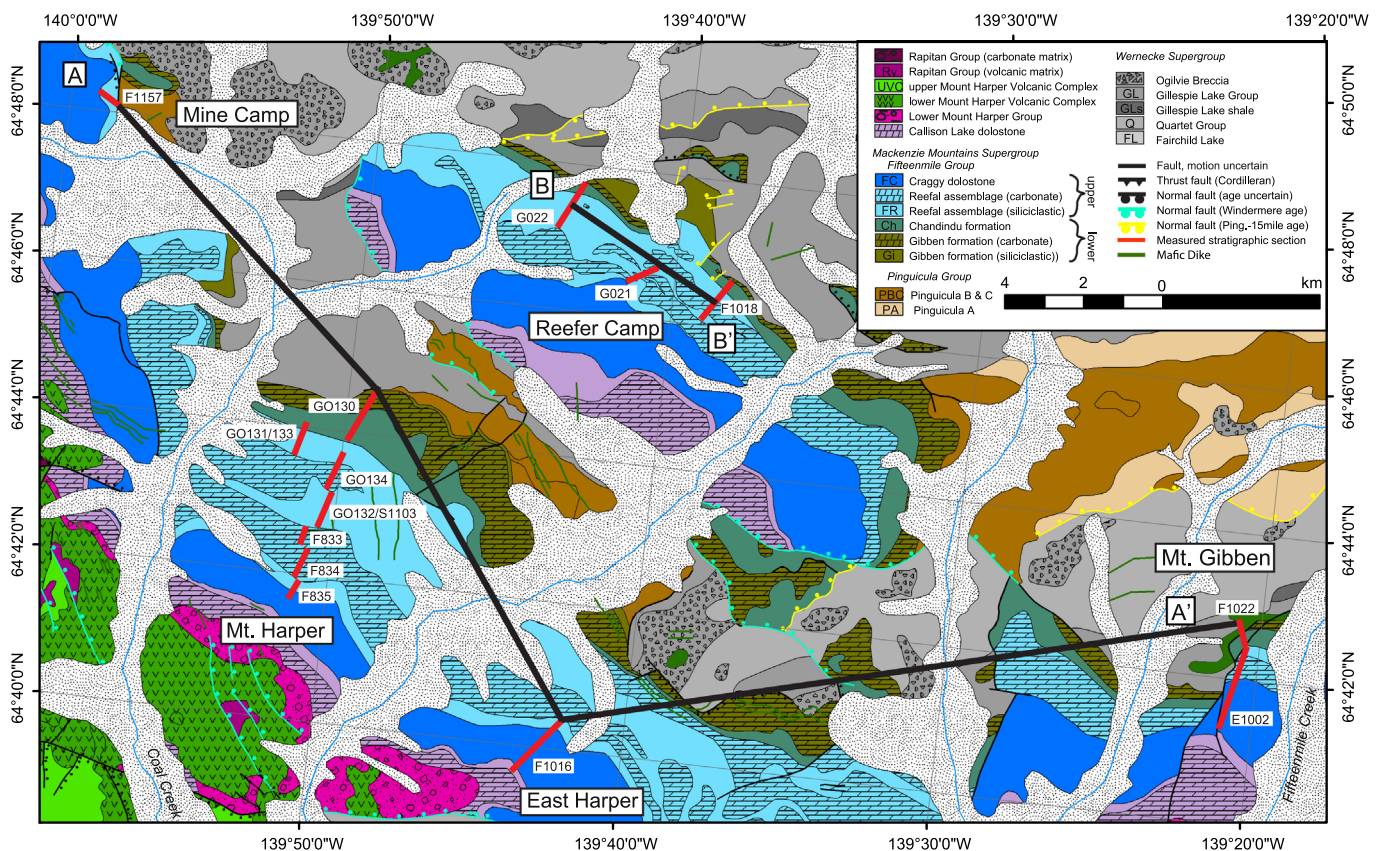


Fig. 2. Geological map of the Coal Creek inlier, Ogilvie Mountains, Yukon Territory, showing sections (in red) studied in this paper. The stratigraphic framework for basin transects A–A' and B–B' are found in Figs. 3 and 4. The units studied as part of this paper are the informal Gibben formation, Chandindu formation and Reefal Assemblage of the Fifteenmile Group. Geological mapping by Macdonald et al. (2012). (For interpretation of the references to color in this figure legend, the reader is referred to the web version of this article.)

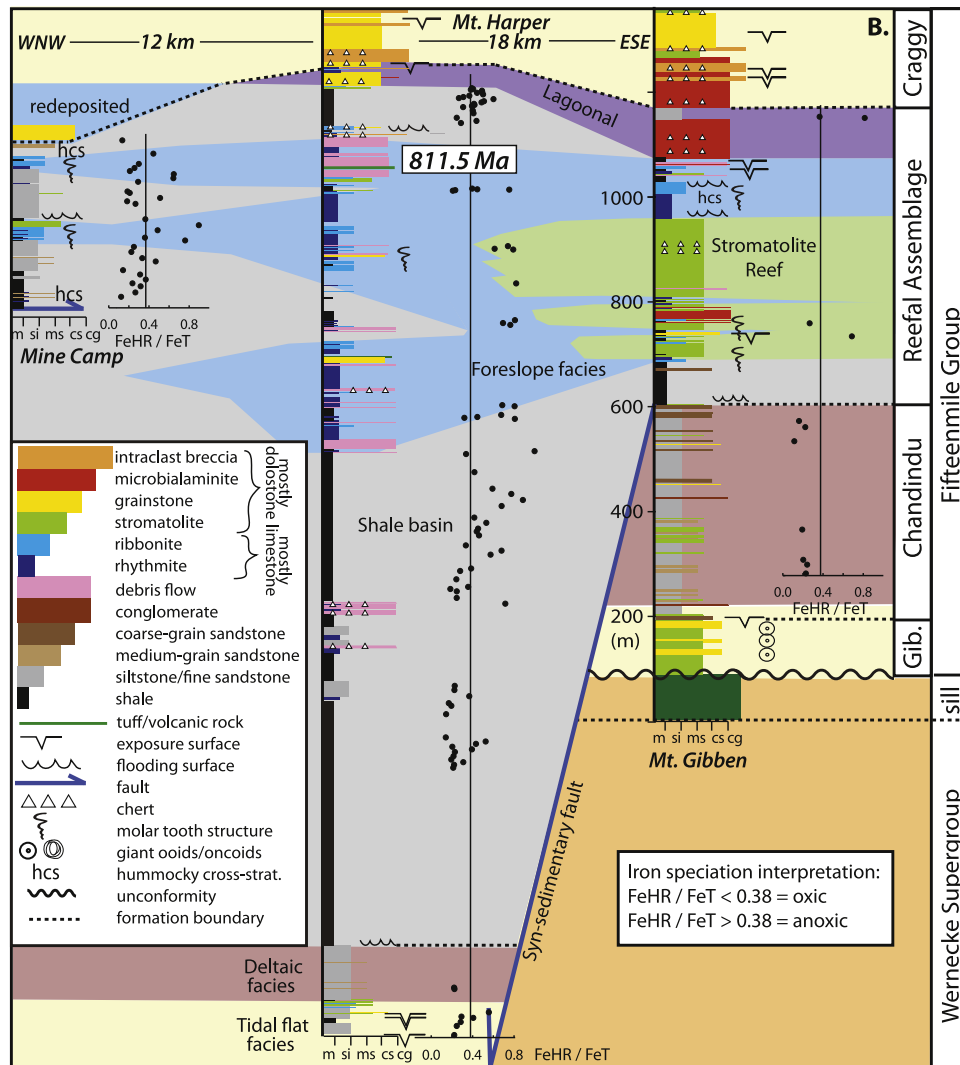


Fig. 3. Stratigraphic framework and iron speciation chemistry for transect A–A' at Mine Camp, Mt. Harper and Mt. Gibben, Coal Creek inlier. Iron speciation chemistry (specifically the ratio of highly reactive iron (FeHR) to total iron (FeT)) from fine-grained siliciclastic rocks is plotted against the stratigraphic columns. Vertical line on iron speciation plots denotes a ratio of 0.38, with samples having higher ratios considered to have been deposited under an anoxic water column, and samples with lower ratios likely to have been deposited under an oxic water column. Complete redox proxy data for individual sections are found in Fig. 6 (Mt. Harper), Supplementary Fig. S1 (Mine Camp), Supplementary Fig. S2 (East Harper) and Supplementary Fig. S3 (Mt. Gibben). *m*—mud; *si*—silt; *ms*—medium sand; *cs*—coarse sand; *cg*—conglomerate. *Gib.* = Gibben formation. (For interpretation of the references to color in this figure, the reader is referred to the web version of this article.)

data can then be placed in the context of other information constraining Mesoproterozoic and early Neoproterozoic oxygen levels and compared to the likely physiological requirements of early animals.

2. Geologic background

Neoproterozoic strata in the northern Canadian Cordillera are exposed in erosional windows ('inliers') separated by Phanerozoic cover (Rainbird et al., 1996; Thorkelson et al., 2005) (Fig. 1). In the Coal Creek inlier, the focus of this study, geological mapping (Fig. 2) and stratigraphic analysis indicate that Neoproterozoic extension produced a series of NNW-side down normal faults, such that the basin, at least locally, deepened toward the northwest in present-day coordinates (Macdonald et al., 2012). The Fifteenmile Group consists of lagoonal, tidal, and supertidal carbonates of the informal Gibben formation, tidal flat and deltaic deposits of the Chandindu formation, and mixed carbonates and siliciclastics of the Reefal Assemblage, which is characterized by km-scale stromatolitic reefs that transition laterally into shale-dominated, deeper water sub-basins (Macdonald et al., 2012).

Shales were sampled from two parallel transects across the basin (Fig. 2), including a shorter transect passing a short distance from a stromatolite reef complex into the shale basin (Fig. 4), and a longer transect stepping further into the basin (Fig. 3). Shales were also investigated from exposures of the Reefal Assemblage ~75 km to the northwest in the Tatonduk inlier that have yielded distinctive scale microfossils (Cohen et al., 2011; Cohen and Knoll, 2012). As Fifteenmile Group strata in the Tatonduk inlier are represented only by shale interbedded with re-deposited carbonate (and no evidence for shallow-water sedimentation), these exposures are interpreted to have formed in a deeper, more distal environment than correlative sections in the Coal Creek inlier (Macdonald et al., 2012); however, displacement along poorly exposed post-Jurassic faults between the two inliers precludes precise paleogeographic reconstruction.

3. Materials and methods

Two hundred and thirty-four shale samples from logged stratigraphic sections were crushed to flour and analyzed for major and

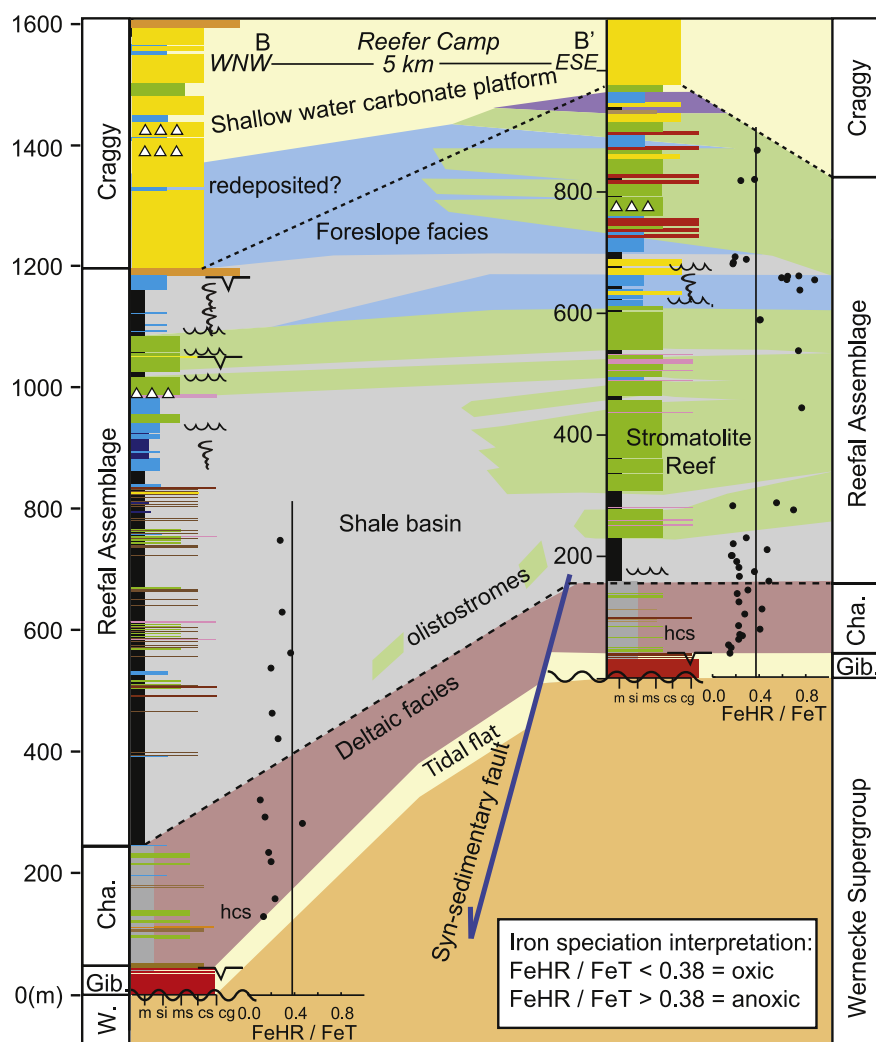


Fig. 4. Stratigraphic framework and iron speciation chemistry for transect B–B' at Reefer Camp, Coal Creek inlier. Sections are located 5 km apart and record a transition in the Reefal Assemblage from a stromatolite reef complex into a deeper-water shale basin. Iron speciation chemistry (specifically the ratio of highly reactive iron (FeHR) to total iron (FeT)) from fine-grained siliciclastic rocks is plotted against the stratigraphic columns. Vertical line on iron speciation plots denotes a ratio of 0.38, with samples having higher ratios considered to have been deposited under an anoxic water column, and samples with lower ratios likely to have been deposited under an oxic water column. Complete redox proxy data for individual sections at Reefer Camp is found in Fig. 5. Legend for stratigraphic columns and sediment type abbreviations as in Fig. 3. Abbreviations: W. = Wernecke Supergroup, Gib. = Gibben formation, Cha. = Chandindu formation.

minor-element concentrations, iron speciation systematics, percent carbonate carbon and organic carbon, and pyrite sulfur isotope composition. Iron sequential extraction followed standard protocols for iron carbonate, iron oxide and magnetite extractions (Poulton and Canfield, 2005), while pyrite iron content was quantified using the chromous chloride extraction method (Canfield et al., 1986). Pyrite sulfur isotopes were determined through combustion via a Costech Elemental Analyzer linked to a Thermo Scientific Delta V in continuous flow mode (measured as $\text{SO}-\text{SO}_2$) using Ag_2S from the chromous chloride extraction. Major- and minor-element abundances were determined following a standard acid digestion (hydrofluoric, perchloric, hydrochloric and nitric) and measurement with ICP-AES at SGS Laboratories, Canada. Percent carbonate carbon was quantified by percent loss on acid dissolution. Total organic carbon values were determined on acidified samples by combustion within a Carlo Erba NA 1500 Analyzer attached to a Thermo Scientific Delta V Advantage isotope ratio mass spectrometer. Complete materials and methods and precision estimates for each analysis are contained in Supplementary information.

4. Results

All geochemical measurements are reported in Supplemental information Tables S1 and S2. Iron speciation data are plotted against the sequence stratigraphic framework for the Coal Creek inlier (Macdonald et al., 2012) in Figs. 3 and 4. Full redox proxy data are plotted against stratigraphy for the principal investigated sections including the short transect at Reefer Camp (Fig. 5), the long transect at Mt. Harper (Fig. 6), and the deepest-water section at Mt. Slipper (Fig. 7). Similar plots for sections with more limited data in the Coal Creek inlier (Mine Camp, East Harper and Mt. Gibben) can be found in Supplementary Figs. S1, S2 and S3, respectively.

4.1. Multi-proxy estimation of paleo-redox state

An estimate of water-column redox state was determined using a multi-proxy approach based on iron speciation chemistry, redox-sensitive trace elements (especially Mo and V) and pyrite sulfur isotope values. In iron speciation chemistry, the highly-reactive

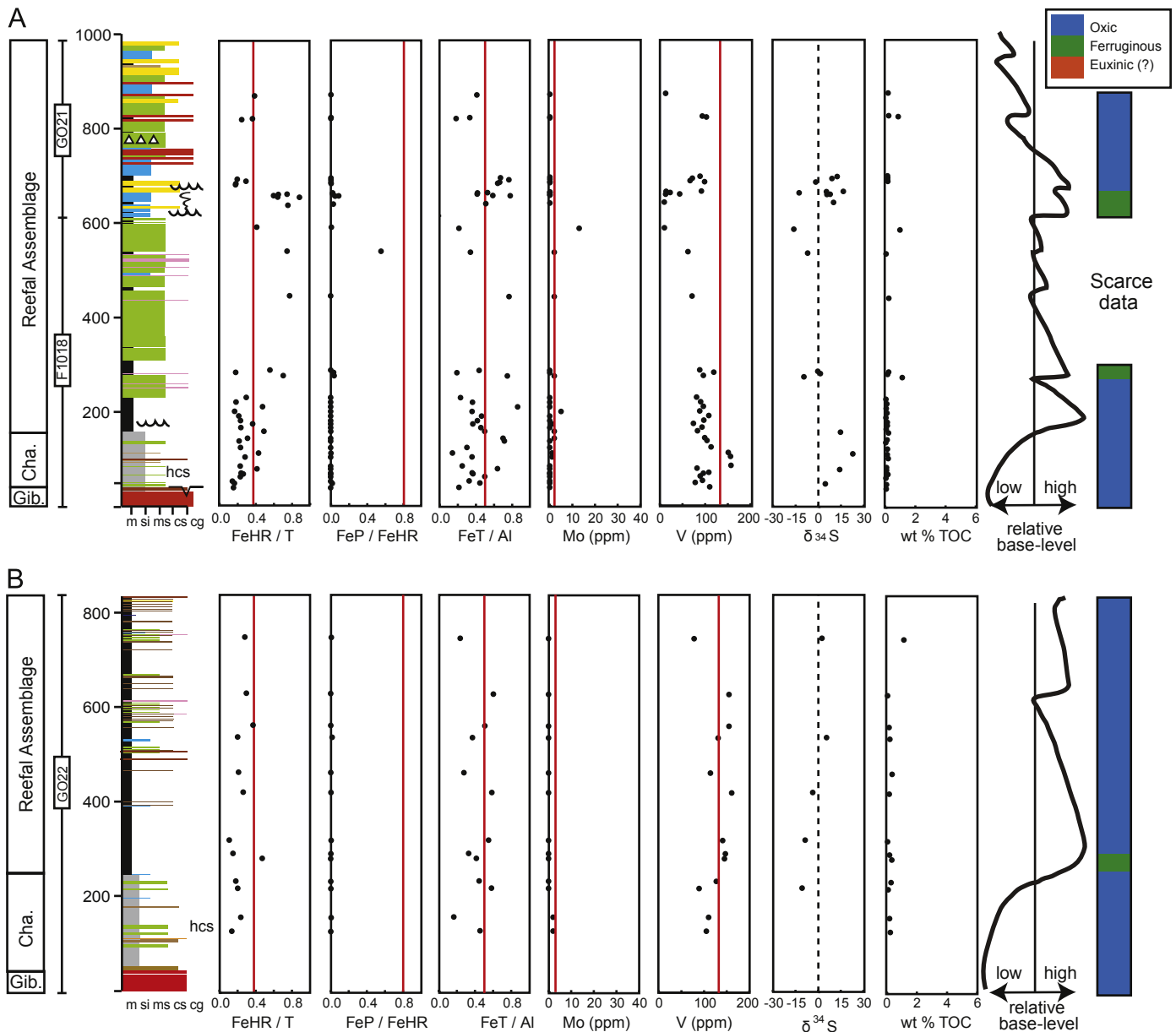


Fig. 5. Redox proxy data from sections B' (A) and B (B) at Reefer Camp, Coal Creek inlier. From left to right, proxy data plotted and their respective relevant baseline data denoted by vertical red lines are highly reactive to total iron (FeHR/FeT; 0.38), pyrite iron to highly reactive iron (FeP/FeHR; 0.80), average shale total iron to total aluminum (FeT/Al; 0.50), average shale molybdenum (2.6 ppm), average shale vanadium (130 ppm), pyrite sulfur isotope values (‰), and weight percent total organic carbon. Relative base level curve from sequence stratigraphic study of Macdonald et al. (2012). The far right column is a subjective estimate of water column redox status based on the multi-proxy data, and is meant to represent general trends rather than an estimate for every point. Euxinia(?) denotes uncertainty regarding whether these samples represent deposition under a truly euxinic water column or a ferruginous water column with sulfide production at or near the sediment–water interface (see text). Legend for stratigraphic column and formation name abbreviations as in Figs. 3 and 4. (For interpretation of the references to color in this figure legend, the reader is referred to the web version of this article.)

pool (FeHR) consists of iron in pyrite (FeP) plus iron that is reactive to sulfide on early diagenetic timescales (iron carbonates such as siderite and ankerite, and iron oxides, including magnetite). The remaining unreactive pool (FeU) consists mainly of iron in sheet silicates; the sum of the two pools is total iron (FeT). Key to the geological application of this proxy is the observation that modern sediments deposited under oxic water columns have a FeHR/FeT < 0.38, while those deposited beneath anoxic water masses generally have FeHR/FeT > 0.38 (Raiswell and Canfield, 1998; see also Farrell (2011), and Supplementary information for further discussion). The proxy can also distinguish the nature of an anoxic water column based on the proportion of highly reactive iron that has been sulfidized, with FeP/FeHR ratios > 0.80 indicating an euxinic water column, and lower ratios pointing toward

ferruginous conditions (Anderson and Raiswell, 2004; Poulton and Canfield, 2011).

Like all proxies, iron speciation has acknowledged caveats. For instance, dilution by turbidites or rapid sedimentation can result in low FeHR/FeT ratios, imparting a false oxic 'signature' to sediments deposited under an anoxic water column (Raiswell and Canfield, 1998; Lyons and Severmann, 2006). Near-shore or estuarine sediments can trap large amounts of iron oxides, leading to an anoxic FeHR/FeT signature for sediments deposited under oxic conditions (Poulton and Raiswell, 2002). Weathering can oxidize Fe²⁺ phases to Fe³⁺ phases, potentially skewing the interpretation of euxinic versus ferruginous conditions (see below), although the FeHR term should remain constant (Canfield et al., 2008). Consistency between independent proxies is the best test of an inference, and consequently

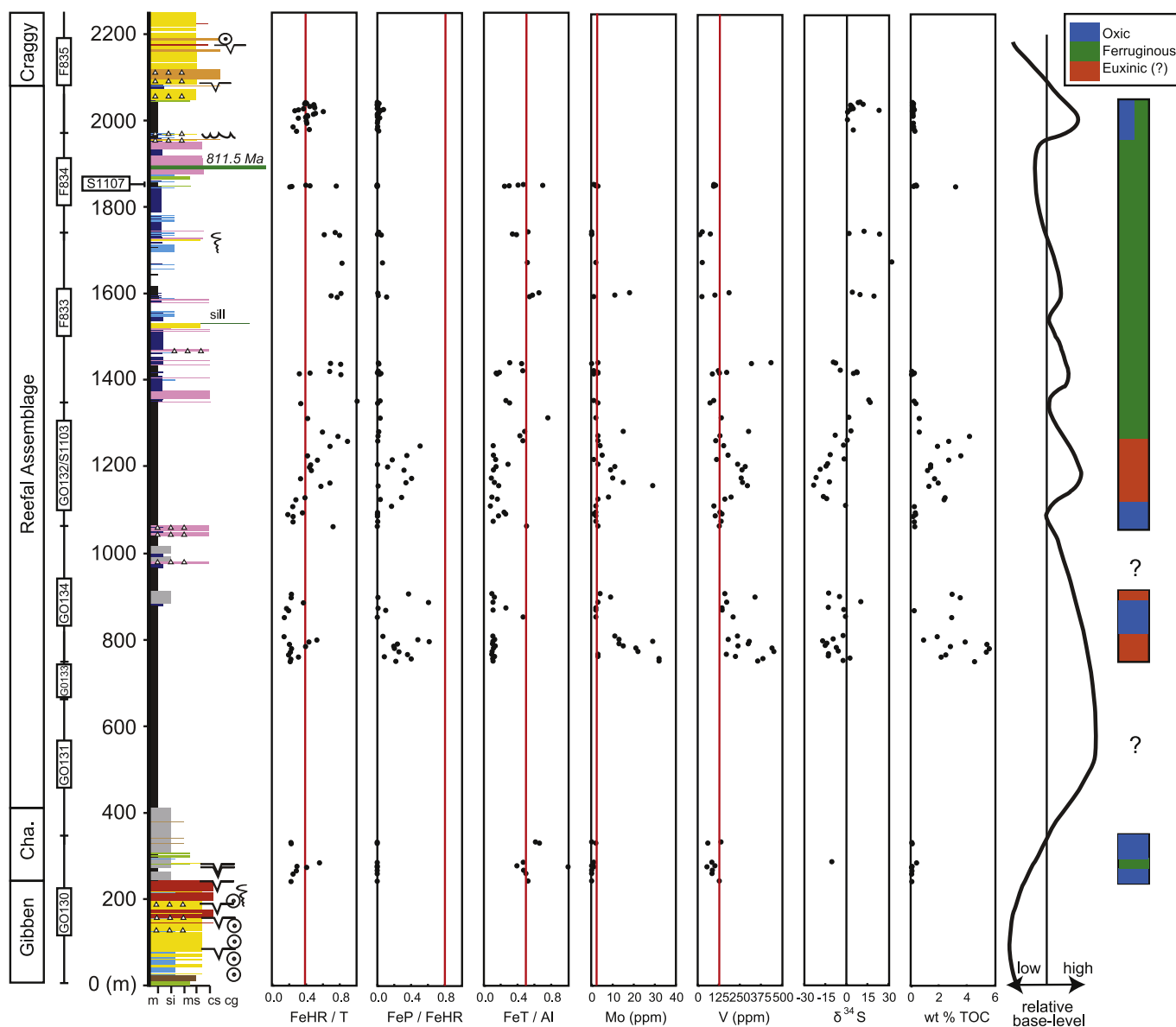


Fig. 6. Redox proxy data from the Mt. Harper section, Coal Creek inlier. This figure is a composite section from the Mt. Harper area (Fig. 2). Redox proxy data and their relevant baseline values (marked by vertical red lines) as in Fig. 5. Relative base level curve from sequence stratigraphic study of Macdonald et al. (2012). The far right column is a subjective estimate of water column redox state based on the multi-proxy data, and is meant to represent general trends rather than an estimate for every point. Euxinia (?) denotes uncertainty regarding whether these samples represent deposition under a truly euxinic water column or a ferruginous water column with sulfide production at or near the sediment–water interface (see text). Legend for stratigraphic column and formation name abbreviations as in Figs. 3 and 4. (For interpretation of the references to color in this figure legend, the reader is referred to the web version of this article.)

we integrated the iron speciation chemistry with other redox proxies and sedimentological constraints. Redox-sensitive trace elements such as vanadium and molybdenum are soluble under oxic conditions but are less soluble under reducing conditions, and are scavenged by organic and inorganic particles or complex with sulfide, leading to enrichments compared to average shale values (Tribouillard et al., 2006). Pyrite sulfur isotope values can further inform paleoenvironmental reconstruction, because sulfate reduction within a water-column where sulfate is not limiting allows expression of the biological preference for lighter ^{32}S , and consequently depleted isotopic compositions in the resulting pyrite with respect to seawater sulfate. Sulfate reduction within sediments, on the other hand, where sulfate availability is often diffusion limited, results in Rayleigh distillation, leading to pyrite values that approach seawater sulfate (Johnston and Fischer, 2012).

In our multi-proxy framework, samples were considered likely to have been deposited under an oxic water column when they

showed $\text{FeHR}/\text{FeT} < 0.38$ (Raiswell and Canfield, 1998), no enrichment in Mo and V with respect to average shales (Gromet et al., 1984), and relatively enriched $\delta^{34}\text{S}$ pyrite sulfur isotope values (or not enough sulfide present in the rock for measurement). Samples were considered to have been deposited under an anoxic, ferruginous water column when they showed $\text{FeHR}/\text{FeT} > 0.38$, little to no Mo enrichment but often with V enrichment, and relatively enriched $\delta^{34}\text{S}$ pyrite sulfur isotope values. Finally, samples were considered to have been likely deposited under an anoxic, euxinic water column when they showed $\text{FeHR}/\text{FeT} > 0.38$, relatively high FeP/FeHR ratios, Mo and V enrichments, and depleted $\delta^{34}\text{S}$ pyrite sulfur isotope values.

Euxinic water columns are usually distinguished by $\text{FeP}/\text{FeHR} > 0.80$ or 0.70 (Poulton and Canfield, 2011), a ratio which few of these samples surpasses. Samples interpreted here as euxinic, though, clearly have much higher FeP/FeHR ratios than samples interpreted as ferruginous (see Figs. 6 and 7), and essentially no

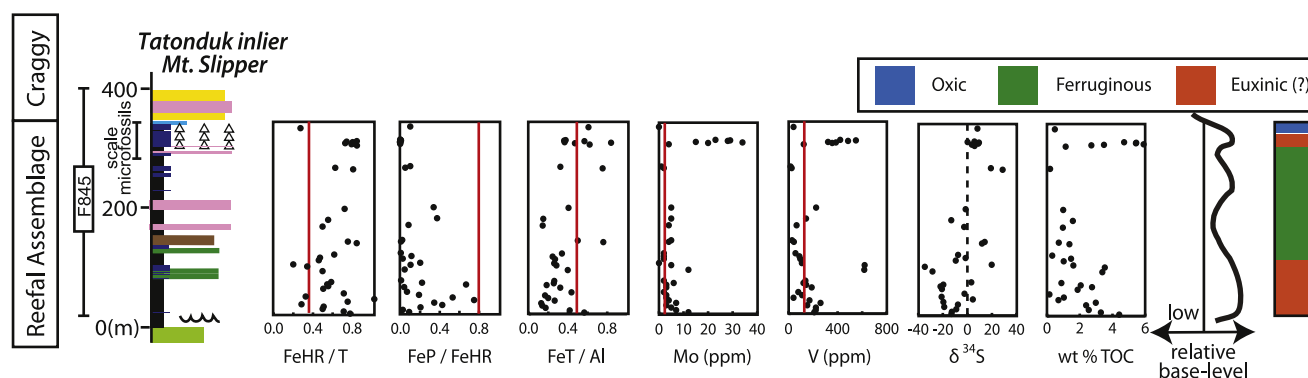


Fig. 7. Redox proxy data from the Mt. Slipper section, Tatonduk inlier. Redox proxy data and their relevant baseline values (marked by vertical red lines) as in Fig. 5. Relative base level curve from sequence stratigraphic study of Macdonald et al. (2012). The far right column is a subjective estimate of water column redox state based on the multi-proxy data, and is meant to represent general trends rather than an estimate for every point. Euxinia(?) denotes uncertainty regarding whether these samples represent deposition under a truly euxinic water column or a ferruginous water column with sulfide production at or near the sediment–water interface (see text). Legend for stratigraphic column and formation name abbreviations as in Figs. 3 and 4. Scale microfossils described by Cohen et al. (2011) are found at the top of the Reefal Assemblage at this locality. (For interpretation of the references to color in this figure legend, the reader is referred to the web version of this article.)

iron carbonate or magnetite. Further, these shales have very depleted $\delta^{34}\text{S}$ pyrite sulfur isotopes (to -34%) and high molybdenum abundances relative to other Neoproterozoic samples (Scott et al., 2008). Two likely possibilities exist to explain these patterns: (1) these shales were deposited beneath an euxinic water column, with subsequent oxidation of pyrite to iron oxides, or (2) the shales were deposited beneath a ferruginous water column, with the zone of free sulfide accumulation essentially at the sediment–water interface. Petrographic examination of selected shales did not show widespread evidence for oxidation of pyrite, although because the samples are from outcrop and surely have suffered some alteration, it is possible that micron-scale pyrite grains beneath the limits of routine petrographic detection have been wholly or partially oxidized. In the second possibility, full access to seawater sulfate and molybdenum pools could explain the isotopic and abundance patterns for these two elements, while the shorter time interval exposed to high sulfide levels compared to a fully euxinic water column would result in less sulfidization of highly-reactive iron phases. Recognizing that the development of truly euxinic conditions is ambiguous and these data may represent sulfide production at the sediment–water interface, inferences of euxinia in Figs. 5–7 should be treated with caution.

4.2. Sedimentary geochemistry of the Fifteenmile Group

4.2.1. Reefer Camp transect, Coal Creek inlier

Near Reefer Camp, samples from the shallow-water Chandindu formation show the hallmarks of deposition under an oxic water column (Fig. 5A). Within the stromatolite reef core of the Reefal Assemblage, thin black shales show high FeHR/FeT, but because they show no redox-sensitive trace element enrichment, and the FeHR signal is entirely dominated by iron oxides, this may represent nearshore trapping of oxides, as occurs in modern settings (Poulton and Raiswell, 2002) rather than a true ocean redox signal. Samples above the flooding surface atop the stromatolite reef tract have iron speciation values persistently above 0.38, moderate amounts of iron carbonate, no Mo enrichment and enriched pyrite sulfur isotope values, pointing to deposition under ferruginous conditions. Samples from the upper part of the Reefal Assemblage signal an apparent return to oxic deposition. In Fig. 5B (see Fig. 4 for the stratigraphic relationship of these sections), the Chandindu formation samples again show evidence for oxic deposition. Continuing upsection into shale of the Reefal Assemblage, all available evidence points to deposition under a generally oxic water column.

4.2.2. Mt. Harper, Coal Creek inlier

Near Mt. Harper, shallow-water sediments of the Chandindu formation also show evidence for oxic deposition (Fig. 6). The Mt. Harper transect steps much farther westward into the Reefal Assemblage shale basin than the short transect at Reefer Camp, and records a thick package of black shale and foreslope carbonate that fill accommodation space associated with tectonic extension (Macdonald et al., 2012). In section G0134, the stratigraphically lowest exposed shales of the Reefal Assemblage, there is evidence for euxinic deposition. Many of these samples do not show FeHR/FeT > 0.38 , but as this succession contains many siltstone turbidites and redeposited carbonates and was likely deposited rapidly during active extension (Macdonald et al., 2012), it is possible that the highly-reactive iron was diluted by high sedimentation rates. Thus a threshold for anoxia of 0.22 may be more appropriate (Raiswell and Canfield, 1998; see also discussion in Supplementary information). These samples show relatively high FeP/FeHR, high Mo (~ 10 – 32 ppm; high for Neoproterozoic shales—Scott et al., 2008), and depleted pyrite sulfur isotope values, indicating sulfide production very near to the sediment–water interface, if not in the water column (see above). The upper half of section G0134 shows lower Mo and less depleted pyrite sulfur isotope values, potentially suggesting ferruginous or even oxic conditions. Samples at the base of section S1103 have FeHR/FeT < 0.38 , no redox-sensitive trace element enrichments, and no pyrite, possibly recording deposition under oxic conditions. This is followed by a second pulse of euxinic deposition, showing similar characteristics to the samples in G0134, with elevated FeP/FeHR, high Mo abundances, and depleted pyrite sulfur isotope values. There is little evidence for euxinia above this level, with ferruginous conditions dominant in the upper Reefal Assemblage. In contrast to samples from the lower Reefal Assemblage at Mt. Harper, where the FeHR pool is almost entirely in pyrite and iron oxides, samples from the upper Reefal Assemblage contain moderate quantities of iron carbonate. In combination with low Mo, and enriched and variable pyrite sulfur isotope values, this suggests that the upper half of the Reefal Assemblage accumulated under an anoxic, ferruginous water column. Brief and fluctuating water column oxygenation may have occurred, as evidenced by stratigraphically-variable iron speciation signatures.

4.2.3. Mt. Slipper, Tatonduk inlier

Iron speciation values from the Reefal Assemblage in the Tatonduk inlier (Fig. 7), which represent the deepest-water setting studied (Macdonald et al., 2012), generally show FeHR/FeT > 0.38 ,

indicating persistent deposition under an anoxic water column. Samples from the base of the section have relatively high FeP/FeHR, high Mo and depleted pyrite sulfur isotope values, pointing to euxinic deposition (or at least fluctuating euxinia). At ~90 m, these proxy values decrease, indicating a transition to ferruginous conditions. A possible return to euxinia is seen at the top of the section, from strata that have yielded scale microfossils (Cohen et al., 2011).

4.2.4. Sediment total iron contents

The total iron to aluminum ratio is another informative redox proxy, because sedimentary iron is authigenically enriched under anoxic water columns (Lyons and Severmann, 2006). An interesting feature of shale samples from the Fifteenmile Group is that even samples considered to have been deposited under anoxic conditions have Fe/Al ratios lower than average shale (Gromet et al., 1984). Given the general concordance in these samples of FeHR/FeT, redox-sensitive trace element abundances and pyrite sulfur isotope data, the inconsistency with Fe/Al likely indicates an intrinsic bias to either total iron or total aluminum in the Reefal Assemblage, rather than this representing oxic deposition. Total Al abundances in all shales investigated (average = 7.03 wt%) are slightly depressed relative to the North American Shale Composite (NASC; Gromet et al., 1984; 8.94 wt%). In contrast, total Fe (average = 2.43 wt%) is significantly reduced relative to NASC (4.43 wt%), especially considering that basal samples interpreted as anoxic should be enriched in iron. Some Reefal Assemblage shales are exceptionally low in total iron (< 1 wt%), and have very high FeHR/FeT ratios indicating a near-absence of detrital iron-silicates. Dilution by carbonate may explain some of the low iron contents, as some samples are slightly calcareous (to ~30–40%, average $9.45 \pm 9.50\%$, Supplementary Table 1) but low iron contents persist in shale samples that have essentially no carbonate (e.g. G0134 and S1103 sections). Open-system diagenesis could have potentially affected these rocks, although even the marls would have had very low permeability. Further, the main effect of diagenesis in carbonates is to add iron (Brand and Veizer, 1980), which is unlikely given the low overall amounts of acetate-extractable iron (average 0.13 wt%) and the lack of a relationship between percent carbonate and acetate-extractable iron ($R^2 = 0.062$). Another possibility is that the provenance was extremely weathered, iron-free material. However, Chemical Index of Alteration (CIA; Nesbitt and Young, 1982) values average ~70 throughout the dataset, indicating a fairly unweathered provenance. A few values in the 75–85 range suggest a weathered source for those samples, but overall there is no obvious correlation between CIA and total iron. Thus, while several factors may explain some low iron values, none can explain all low values. We note that some other Neoproterozoic sections show anomalously low FeT/Al (e.g. Sahoo et al., 2012); further study is needed to determine if these are local, basin-level effects or an as-yet-unexplained aspect of the Neoproterozoic iron cycle.

4.2.5. Redox proxy data and sediment organic carbon contents

Sediment TOC results vary consistently compared to multi-proxy inferences of redox state (Fig. 8). Sediments likely deposited under an oxic water column have low organic carbon abundances (average = $0.31\% \pm 0.49$ wt%; median = 0.19%), whereas those inferred to have been deposited beneath a ferruginous water column have higher sediment TOC values (average = $0.66\% \pm 1.37$; median = 0.28%). And sediments likely deposited beneath euxinic conditions show much greater TOC (average = $2.87\% \pm 1.49$; median = 2.63). Thus, these data are consistent with the hypothesis that the development of euxinic conditions in Neoproterozoic basins is primarily driven by the degree of organic carbon loading and the exhaustion of more energetically-favorable electron acceptors than sulfate (e.g. Fe^{3+}) (Johnston et al., 2010).

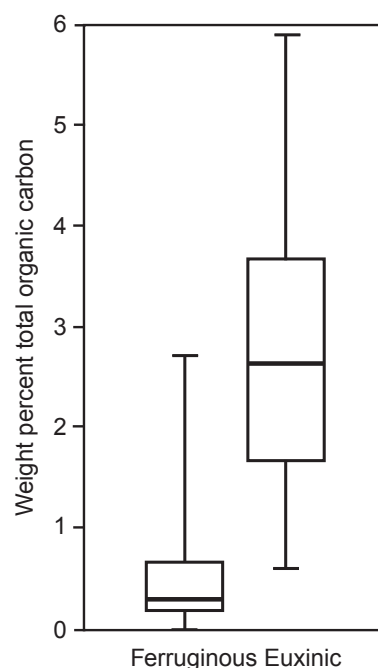


Fig. 8. Boxplot analysis of total organic carbon weight percentages for samples determined likely to have been deposited under a ferruginous and euxinic water column. Bottom-water redox state for each sample was estimated using a multi-proxy framework including iron speciation data, redox-sensitive trace elements and pyrite sulfur isotope values (see text for details). Samples designated as euxinic may represent sulfide accumulation at the sediment–water interface rather than true water-column euxinia (see text). The box represents the 25th and 75th percentiles, the thick horizontal line represents the median, and the whiskers represent minimum and maximum values. An extreme outlier in the ferruginous set (E1002-470.4; 9.87 wt%) was included in the boxplot calculations but not graphed.

4.2.6. Redox proxy data and water depth

Redox proxy data show a consistent pattern with respect to sedimentological structures that indicate relative water depth. In particular, samples in association with all occurrences of wave-generated sedimentary structures, including hummocky cross-stratified sandstones encased in shale, which indicate deposition above storm wave base, show evidence for oxic deposition (Figs. 3–7). In other words, the surface mixed layer in the basin appears to be oxygenated, at least during storms. While the depth of storm wave base varies among basins (Peters and Loss, 2012), these data indicate that in this basin, the water column in direct contact with the atmosphere remained oxic. Oxygenated conditions may extend slightly deeper, as some sediments likely deposited below storm wave base (such as shales basinward of the stromatolite reef at Reefer Camp, Fig. 5B) still indicate oxic conditions. A few brief intervals of oxygenated conditions, or fluctuating anoxia, persist deeper into the Coal Creek inlier shale basin as recorded in the Mt. Harper (Fig. 6) and Mine Camp (Supplementary Fig. S1) sections, but the majority of these deeper-water sediments record anoxic conditions. The deepest-water section at Mt. Slipper in the Tatonduk inlier (Fig. 7), which shows no evidence for wave activity, is persistently anoxic. Thus, there is a clear redox structure to the basin, with an oxygenated surface layer where the sediments are in contact with the atmosphere (storm wave base), and anoxic conditions below this depth.

5. Discussion

5.1. Fifteenmile Group redox structure in a global context

Quantitative constraints on Proterozoic oxygen levels are notoriously difficult to obtain (Kump, 2008). O_2 levels in the

mid-Proterozoic must have been above 0.001% present atmospheric levels (PAL), the limit imposed by the disappearance of mass-independent fractionation of sulfur isotopes at ~ 2.45 Ga (Farquhar et al., 2000; Pavlov and Kasting, 2002). Two other constraints have been proposed for mid-Proterozoic O_2 (Kump, 2008). First, anoxic deep oceans likely require atmospheric O_2 to be less than 40% PAL (Canfield, 2005). Second, it has been proposed that iron is only retained in lithified soil horizons, and it has been since the Paleoproterozoic, when O_2 is greater than 1% PAL (Holland and Beukes, 1990). These limits on Proterozoic O_2 have caveats, and it has even been hypothesized that levels may not have been dramatically different from the Phanerozoic (Butterfield, 2009). Nonetheless, it is notable that the basin redox transect of the Fifteenmile Group is consistent with proposed quantitative limits (Kump, 2008). Indeed, the basin redox structure of the Fifteenmile Group is similar in many ways to that of the Mesoproterozoic Roper Group in Australia (Shen et al., 2003), with an oxygenated shelf overlying anoxic basinal waters. Although there are local drivers for anoxia (Tyson and Pearson, 1991), the available basin redox transects point to extensive subsurface anoxia in the Proterozoic oceans, sustained over hundreds of meters of stratigraphic section. This clearly differs from Phanerozoic ocean anoxic events (Campbell and Squire, 2010), indicating a different driver and implying lower atmospheric O_2 than the modern. Placing minimum constraints on global atmospheric pO_2 levels from local iron speciation data is difficult, but shallow-water facies in the Fifteenmile Group record oxic deposition, as do samples from the shale basin just off the reef margin at Reefer Camp (Fig. 5), and some samples from deeper in the shale basin at Mt. Harper (Fig. 6) and Mine Camp (Supplementary Fig. S1), implying enough atmospheric oxygen to counteract strong benthic reductant fluxes in a basin otherwise prone to euxinia (cf. Kump et al., 2005).

In sum, although there is clear need to study more basins, and develop new global redox proxies and models, the basin redox transect of the Fifteenmile Group is consistent with proposed constraints on Proterozoic oxygen levels as being $< 40\%$ and $> 1\%$ PAL (Kump, 2008). We apply these bounds for comparison with the physiological requirements of early animals.

5.2. Physiological requirements of early animals

The consistency of previously proposed constraints on atmospheric oxygen with the basin redox transect of the Fifteenmile Group prompts the question of whether such oxygen levels would have prohibited the evolution of animal, eumetazoan or bilaterian body plans. A common assumption in attempts to link late Precambrian oxygenation and biospheric evolution is that animals have high respiratory demands. While metazoans do have a clear and definite requirement for oxygen, they are not a monolithic group, and the oxygen requirements for any given organism varies widely based on size, metabolism, and the presence or absence of a circulatory system (Vaquer-Sunyer and Duarte, 2008). Hypotheses relating geochemical change to early animal evolution must therefore compare inferred changes against the explicit body plans, ecological strategies and taxonomic groups presumed to be affected. Determining the physiological requirements of ancient organisms has obvious uncertainty, but can be accomplished through analogy with living representatives (Knoll et al., 2007), and thus it is possible to make general statements about the likely oxygen requirements of Precambrian animals.

5.2.1. Diploblastic metazoans

Whether sponges are monophyletic (Philippe et al., 2009) or paraphyletic (Sperling et al., 2009), they are certainly the sister group or grade of all other animals (Philippe et al., 2011). Moving up the metazoan phylogenetic tree, the exact relationships of

cnidarians, ctenophores and placozoans to bilaterians are unclear, but all are likely more closely related to bilaterians than they are to sponges (Philippe et al., 2011). Importantly, all these animals (diploblasts) are characterized by only two epithelial cell layers, with the space between layers filled largely with metabolically-inert material (e.g. mesohyl in sponges, mesoglea in cnidarians). From a respiratory point of view, then, essentially every cell in a diploblastic metazoan is in direct contact with seawater (Ruppert et al., 2004). Thus, the theoretical oxygen limit for diploblastic animals will not differ from that of a single-celled eukaryote, barring two minor differences. First, for unicellular eukaryotes, diffusion of oxygen into the cell can occur across the entirety of its surface, whereas diffusion into a sheet of cells cannot occur at cell-cell contacts. Second, animals have a collagenous extracellular matrix, and molecular oxygen is required for the formation of hydroxyproline in collagen (Fujimoto and Tamiya, 1962; Prockop et al., 1963). Using the K_m for the proline hydroxylase system of chick embryos, Towe (1970) suggested oxygen levels of $\sim 3\%$ PAL would be required for collagen synthesis. However, Rhoads and Morse (1971) cogently noted that collagen-rich invertebrates are found at oxygen levels beneath this value (see also discussion below on modern oxygen minimum zones), suggesting that the oxygenase requirements of a terrestrial vertebrate cannot be applied to marine invertebrates. Further, collagen is now known to exist in fungi (Celerin et al., 1996; Wang and Leger, 2006) and choanoflagellates (King et al., 2008—although the homology of both to metazoan collagens remains uncertain), which suggests collagen may have been present in the last common ancestor of opisthokonts. If so, any oxygen requirement for collagen synthesis was met far earlier than the origin of animals.

In the fossil record, clear eukaryotic organisms are found at ~ 1800 Ma, and several lineages of multicellular eukaryotes, which would also have been subject to the same constraint as early animals of limited diffusion at cell-cell contacts, are found in Mesoproterozoic rocks (Runnegar, 1991; Knoll et al., 2006). The presence of these organisms long before the Cryogenian implies that any physiological oxygen threshold for the body plans that characterized the earliest (diploblastic) period of early animal evolution must have been surpassed far prior to the origin of animals themselves.

5.2.2. Bilaterian metazoans—theoretical lower oxygen limits

In contrast to diploblasts, which have sheets of cells separated by inert material, bilaterian (triploblastic) organisms have metabolically-active cells in three-dimensions (Knoll, 2011). Body size (and the ability of the organism to exist at a given oxygen concentration) is consequently limited by the ability to maintain functional internal oxygen levels, either through pure diffusion or through a blood vascular system (BVS). The implications of this constraint under hypothetical Precambrian oxygen levels have been extensively discussed (e.g. Raff and Raff, 1970; Runnegar, 1982a, 1982b, 1991; Catling et al., 2005; Payne et al., 2010). Using a theoretical framework for the diffusion of oxygen into an idealized animal (Alexander, 1971), these studies have demonstrated that low oxygen levels will restrict bilaterians to small, thin body plans. What has not been asked in these theoretical calculations is what oxygen levels will prohibit the existence of bilaterian body plans.

Superficially, this question would seem to hinge on the nature of the last common ancestor of bilaterians (consider Carroll et al. (2001), versus Erwin and Davidson (2002)), specifically whether this ancestor was a complex, coelomate organism with a heart and BVS, or a much simpler organism that transported oxygen through pure diffusion. However, as noted by Budd and Jensen (2000), due to structural size requirements, notably the physical space required to fit a functional BVS, this transport system is generally not present in

modern organisms less than ~ 3 mm in size. Following the framework of Alexander (1971) (see Supplementary information for details), we estimate that the most likely minimal oxygen requirement for a 3 mm-long \times 67 μ m-wide worm with a circulatory system is $\sim 0.14\%$ PAL (Fig. 9). The most likely minimal oxygen requirements for a 600 μ m long \times 25 μ m wide diameter worm limited by pure diffusion is $\sim 0.36\%$ PAL (Fig. 9)—note that these values are with respect to ambient dissolved oxygen concentrations and do not consider temperature or salinity effects on the dissolution of oxygen in water. The estimated oxygen requirements for these two hypothetical ancestors differ slightly, but their broad similarity and the overlap in sensitivity analyses (Fig. 9) suggest that pure diffusion and a BVS likely represent optimal designs below and above this size threshold.

Although there are uncertainties in the optimal values for the parameters in the equations governing oxygen requirements (see Supplementary information), three facts suggest the values described above represent conservative estimates for the minimum oxygen concentrations necessary to sustain bilaterians. First, for the bilaterian limited by pure diffusion, a sensitivity analysis (Fig. 9 and Supplementary Table S7) demonstrates that one of the most important terms at very low oxygen levels is the minimum cellular oxygen concentration. This will be a small, but non-zero, number (Raff and Raff, 1970). Raff and Raff (1970) used a value of 1/10th the shared K_m of yeast and mammalian cytochrome oxidase. Here, rather than adopting an arbitrary but likely more accurate fractional value, we use the shared yeast–mammal K_m (Chance, 1957) as our ‘most likely’ value for this parameter (note that investigated invertebrate cytochrome oxidases have a similar value (e.g. Gnaiger et al., 2000)). This ensures that the most important parameter in the model is an overestimate. Second, for the hypothetical ancestor with a circulatory system, we assumed the organism did not have respiratory pigments. Although the homology of metazoan respiratory pigments is unclear

(Terwilliger, 1998), their presence in this hypothetical last common bilaterian ancestor would greatly increase diffusion rates. Thus, our assumption that respiratory pigments were absent again results in a conservative estimate. Finally, and most importantly, these theoretical calculations assume a perfectly tubular organism (Alexander, 1971). Such an organism does not exist, as real animals have body wall rugosities, gills, and other structures that dramatically increase diffusive surface area with respect to volume; even the gut is a gas-exchange organ. Consequently, these ‘most likely’ values and the sensitivity analyses are not intended to yield a precise number. Rather, these models provide an indication of the lower bound of oxygen levels necessary to preclude the bilaterian body plan from Proterozoic oceans. No matter the complexity of the last common ancestor of bilaterians, theoretical modeling suggests the bilaterian body plan was unlikely to have been prohibited unless O_2 levels were $< 0.4\%$ PAL.

5.2.3. Bilaterian metazoans—empirical lower oxygen limits

These theoretical calculations can be tested with empirical observations of the oxygen limits of bilaterians in modern oxygen-minimum zones (OMZs). Unlike the biota on shelves or in regions of anthropogenic eutrophication that show deleterious oxygen responses at relatively minor oxygen depletions (Diaz and Rosenberg, 1995; Levin et al., 2009), OMZs have experienced geologically long-lasting dysoxic- to anoxic-conditions, allowing the fauna to adapt to these levels and providing an excellent analog for Precambrian oceans with persistently low oxygen levels. It should be noted that organisms in modern OMZs have likely secondarily adapted to these environments rather than originating in them. Thus, the type of adaptations allowing organisms to inhabit these environments must be considered. For example, organisms with extreme metabolic adaptations, such as amitochondriate loriciferans living in an euxinic Mediterranean basin (Danovaro et al., 2010), cannot inform us about Precambrian animal evolution, as the transformation of the mitochondria into a hydrogenosome was certainly not a primitive feature. Most of the adaptations allowing bilaterians to inhabit modern low-oxygen environments, though, appear to lie in their very small, thin body plans (with high surface-area to volume ratios for increased diffusion) and enlarged respiratory organs (Levin, 2003; Gooday et al., 2010; Jeffreys et al., 2012; Lamont and Gage, 2000; Neira et al., 2001)—that is, with morphological adaptations that would have been possible, and perhaps likely, in early bilaterians. Consequently these animals can provide a useful analog for Precambrian animal life in low-oxygen conditions.

In using OMZs as Precambrian analogs, it has long been recognized that the faunas are characterized by such small, thin, body plans (Rhoads and Morse, 1971). What has emerged in the four decades of oceanographic research since Rhoads and Morse’s seminal paper is just how little oxygen is actually required by bilaterian animals. It is now clear that non-chemosymbiotic benthic macrofaunal (retained on 0.3 mm sieves) bilaterians can and do live in Rhoads and Morse’s ‘azoic’ zone of < 0.10 mL/L oxygen¹ (Levin, 2003; Gooday et al., 2010; Levin et al., 2000, 1991, 2002; Palma et al., 2005; Zettler et al., 2009; Ingole et al., 2010), often with densities of hundreds to thousands of animals per square meter. Bilaterian faunas can even be found as low as 0.02 mL/L O_2 , equivalent to $\sim 0.3\%$ of modern surface ocean levels (assuming a normal surface ocean concentration of ~ 6 mL/L) in the OMZ off Chile (Palma et al., 2005), Peru (Levin et al., 2002) and the Bay of Bengal (R. Akkur, pers. comm.). The exact oxygen concentrations

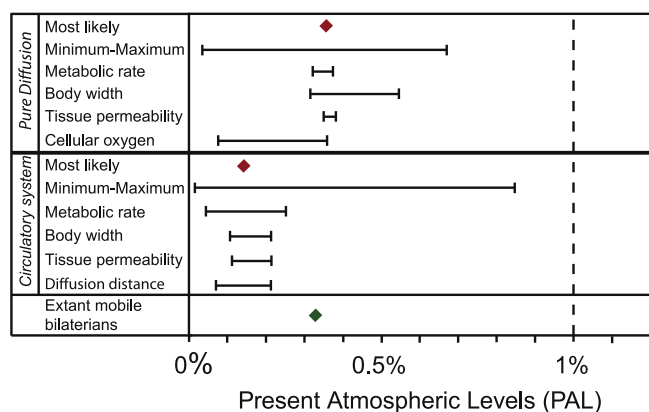


Fig. 9. Theoretical minimum oxygen requirements for the last common ancestor (LCA) of bilaterians, following the equations governing the diffusion of oxygen into an organism from Alexander (1971) and modified by Payne et al. (2010). Estimates were made for two potential body plans characterizing the bilaterian LCA, a 600 μ m long worm limited by pure diffusion, and a 3-mm long worm with a circulatory system. ‘Most likely’ values represent values estimated from optimal values for all parameters (see Supplementary information). Minimum and maximum values were derived from the literature for each parameter and global minimum and maximum values were estimated. A sensitivity analysis was then conducted for each parameter by varying that parameter between minimum and maximum values while keeping all other parameters at their ‘most likely’ values. All estimates for oxygen requirements are far less than the 1% of Present Atmospheric Levels indicated by canonical views of atmospheric oxygen levels in the Proterozoic (Kump, 2008). Lowest row for extant mobile bilaterians shows the current lower oxygen limit at which bilaterians are found in the modern ocean (0.02 mL/L O_2 = 0.33% of modern surface ocean levels assuming a normal surface ocean level of 6 mL/L). Bilaterians are found at these levels off the coasts of Peru, Chile, and in the Bay of Bengal. This oxygen level may represent an overestimate due to the methodology used to measure oxygen in most benthic ecology studies (Breur et al., 2009 and see text).

¹ A difficulty in interdisciplinary research on the biological effects of differing oxygen levels is the use of different units by different research communities (Hofmann et al., 2011). For consistency here we report oxygen levels as in the benthic ecology literature (mL/L). For reference 0.01 mL/L = 0.44 μ mol/kg = 0.014 mg/L = 0.4 atm.

actually required to exclude bilaterians are likely even lower, as these oxygen measurements are determined from O_2 sensors or seawater samples from CTD casts collected several meters (~ 5 m) above the seafloor. The oxygen levels at which bilaterians are recorded (namely 0.02 mL/L) approach the detection limit of the Winkler titration technique (Paulmier et al., 2006), and CTD cast values generally over-estimate in-situ benthic conditions (Breur et al., 2009). Thus, both theoretical calculations and empirical observations in modern OMZs suggest the presence of bilaterians would not have been limited unless atmospheric O_2 was considerably less than 1% PAL, and likely less than 0.4% PAL.

6. Conclusions

Geochemical transects of the ~ 800 Ma Fifteenmile Group in the Ogilvie Mountains document shallow-water facies characterized by low FeHR/FeT, a lack of enrichment in redox-sensitive trace elements, and relatively heavy and variable pyrite sulfur isotope values. Deeper-water facies (those deposited below storm wave base) are characterized by FeHR/FeT > 0.38 , enrichment in redox-sensitive trace elements, and more depleted pyrite sulfur isotope values. Overall, this points toward an oxygenated surface layer, down to storm wave base, overlying a generally anoxic deep basin. Fluctuations between euxinic and ferruginous conditions sub-storm wave base appear to have been controlled by variations in organic carbon loading. As proxies like iron speciation and redox-sensitive trace elements provide evidence of local environments, more geochemical studies from other basins are necessary to begin building the global picture of redox heterogeneity. Further, the development of quantitative global redox tracers and better modeling are needed to place tighter constraints on the history of oxygen on Earth. Nonetheless, the Fifteenmile Group redox structure is comparable to that of a well-characterized Mesoproterozoic basin (Shen et al., 2003)—albeit with more evidence for ferruginous conditions—and both basins are consistent with broad estimates for atmospheric oxygen levels between 1% and 40% PAL (Kump, 2008).

Comparing these likely O_2 levels with the estimated physiological requirements of early animals suggests that sufficient atmospheric oxygen, even for mobile bilaterians, was present well in advance of the origin of animals. Unless early Neoproterozoic oxygen levels were substantially $< 1\%$ PAL, and likely $< 0.4\%$ PAL, atmospheric oxygen levels would not have prohibited the sponge, eumetazoan and bilaterian body plans. This conclusion does not imply that animals necessarily lived in the Fifteenmile basin, but rather that global O_2 levels were likely adequate for the presence of animals. Notably, this does not negate the possibility of an oxygenation event around the Sturtian glaciation (Planavsky et al., 2010; Frei et al., 2009), or the use of oxygenated ‘oases’ beneath photosynthetic mats by the earliest trace makers in the geological record (Gingras et al., 2011), but it does suggest that such conditions were not necessary for the origin of either animals or bilaterians.

It is important to remember, though, that while low Precambrian oxygen levels would not have prohibited animals, including bilaterians, the environmental milieu would still have exerted a strong effect on life. Most importantly, low oxygen certainly would have constrained these organisms to very small and thin body plans with little metabolic scope (Raff and Raff, 1970; Runnegar, 1982a, 1982b; Payne et al., 2010). Faunas in modern low- O_2 OMZ analogs have very small body sizes, reduced diversity, and simple food webs (Levin, 2003; Gooday et al., 2009). In other words, although all available data suggests bilaterians *can* live down to 1% PAL or less, the fauna would be limited to a select few—those organisms that were a couple millimeters in length and had low-

energy lifestyles. Thus, while no oxygenation event need be invoked to explain the origin of animals or bilaterians themselves, the hypothesized end-Neoproterozoic oxygenation event (the timing and magnitude of which remains debated—Kah and Bartley, 2011; Och and Shields-Zhou, 2012) may still have played a role in the later Ediacaran diversification of macroscopic animals and the Cambrian ‘Explosion’ (e.g. Runnegar, 1982a; Rhoads and Morse, 1971; Knoll and Carroll, 1999). Although Cambrian diversification was certainly multifaceted (Erwin et al., 2011), a latest Proterozoic increase in oxygen levels could have allowed for an increase in both size and metabolic scope, including potentially the advent of predation, a metabolically-costly feeding strategy.

Acknowledgments

We thank J. Strauss, A. Eyster, E. Smith and S. Braun for assistance in the field, A. Masterson, E. Beirne, and B. Gill for technical assistance, G. Eischeid, G. Resendiz, D. Cole and N. Waldo for help with sample preparation and laboratory analyses, P. Cohen, P. Girguis, J. Payne, K. Peterson, J. Strauss, L. Levin and C. Frieder for helpful discussion, and D. Fike and two anonymous reviewers for insightful comments. We thank Fireweed Helicopters for safe and reliable transportation, and the Yukon Geological Survey for field support. We thank D. Schrag, Harvard University Laboratory for Chemical Oceanography, and S. Poulton, Newcastle University, for help with sample analysis in their labs. EAS is supported by an Agouron Institute post-doctoral fellowship. DTJ is supported by NSF EAR/IF, NASA Exobiology, and Harvard University. EAS, AHK, DTJ and FAM thank the NASA Astrobiology Institute for support.

Appendix A. Supplementary materials

Supplementary data associated with this article can be found in the online version at <http://dx.doi.org/10.1016/j.epsl.2013.04.003>.

References

- Alexander, R.M.N., 1971. Size and Shape. Edward Arnold, London, pp.1–59.
- Anderson, T.F., Raiswell, R., 2004. Sources and mechanisms for the enrichment of highly reactive iron in euxinic Black Sea sediments. *Am. J. Sci.* 304, 203–233.
- Berney, C., Pawlowski, J., 2006. A molecular time-scale for eukaryote evolution recalibrated with the continuous microfossil record. *Proc. R. Soc. London Ser. B* 273, 1867–1872.
- Brand, U., Veizer, J., 1980. Chemical diagenesis of a multicomponent carbonate system—I: trace elements. *J. Sediment. Petrogr.* 50, 1219–1236.
- Breur, E.R., Law, G.T.W., Wouds, C., Cowie, G.L., Shimmield, G.B., Peppe, O., Schwartz, M., McKinlay, S., 2009. Sedimentary oxygen consumption and microdistribution at sites across the Arabian Sea oxygen minimum zone (Pakistan margin). *Deep-Sea Res. II* 56, 296–304.
- Budd, G.E., Jensen, S., 2000. A critical reappraisal of the fossil record of the bilaterian phyla. *Biol. Rev.* 75, 253–295.
- Butterfield, N.J., 2009. Oxygen, animals and oceanic ventilation: an alternative view. *Geobiology* 7, 1–7.
- Butterfield, N.J., Knoll, A.H., Swett, K., 1994. Paleobiology of the Neoproterozoic Svanbergfjellet Formation, Spitsbergen. *Fossils and Strata* 34, 1–84.
- Campbell, I.H., Squire, R.J., 2010. The mountains that triggered the Late Neoproterozoic increase in oxygen: the second Great Oxidation Event. *Geochim. Cosmochim. Acta* 74, 4187–4206.
- Canfield, D.E., 2005. The early history of atmospheric oxygen: homage to Robert M. Garrels. *Annu. Rev. Earth Planet. Sci.* 33, 1–36.
- Canfield, D.E., Poulton, S.W., Knoll, A.H., Narbonne, G.M., Ross, G., Goldberg, T., Strauss, H., 2008. Ferruginous conditions dominated later Neoproterozoic deep-water chemistry. *Science* 321, 949–952.
- Canfield, D.E., Raiswell, R., Westrich, J.T., Reaves, C.M., Berner, R.A., 1986. The use of chromium reduction in the analysis of reduced inorganic sulfur in sediments and shale. *Chem. Geol.* 54, 149–155.
- Carroll, S., Grenier, J., Weatherbee, S., 2001. From DNA to Diversity: Molecular Genetics and the Evolution of Animal Design. Blackwell Science, Inc., Malden, MA.

- Catling, D.C., Glein, C.R., Zahnle, K.J., McKay, C.P., 2005. Why O₂ is required by complex life on habitable planets and the concept of planetary "oxygenation time". *Astrobiology* 5, 415–438.
- Celerin, M., Ray, J., Schisler, N., Day, A., Stetler-Stevenson, W., Laudenbach, D., 1996. Fungal fibrillae are composed of collagen. *EMBO J.* 15, 4445–4453.
- Chance, B., 1957. Cellular oxygen requirements. *Fed. Proc.* 16, 671–680.
- Cloud Jr, P.E., 1968. Atmospheric and hydrospheric evolution on the primitive Earth. *Science* 160, 729–736.
- Cohen, P.A., Schopf, J.W., Butterfield, N.J., Kudryavtsev, A.B., Macdonald, F.A., 2011. Phosphate biomineralization in mid-Neoproterozoic protists. *Geology* 39, 539–542.
- Cohen, P.A., Knoll, A.H., 2012. Neoproterozoic scale microfossils from the Fifteen-mile Group, Yukon Territory. *J. Paleontol.* 86, 775–800.
- Danovaro, R., Dell'Anno, A., Pusceddu, A., Gambi, C., Heiner, I., Kristensen, R.M., 2010. The first metazoa living in permanently anoxic conditions. *BMC Biol.* 8, 30.
- Diaz, R.J., Rosenberg, R., 1995. Marine benthic hypoxia: a review of its ecological effects and the behavioural responses of benthic macrofauna. *Oceanogr. Mar. Biol. Annu. Rev.* 33, 245–303.
- Erwin, D.H., Davidson, E.H., 2002. The last common bilaterian ancestor. *Development* 129, 3021–3032.
- Erwin, D.H., Laflamme, M., Tweedt, S.M., Sperling, E.A., Pisani, D., Peterson, K.J., 2011. The Cambrian conundrum: early divergence and later ecological success in the early history of animals. *Science* 334, 1091–1097.
- Farquhar, J., Bao, H., Thiemens, M., 2000. Atmospheric influence of earth's earliest sulfur cycle. *Science* 289, 756–758.
- Farrell, U.C., 2011. Taphonomy and Paleocology of Pyritized Trilobite Faunas from Upstate New York. Yale University, New Haven, CT, pp. 1–430.
- Frei, R., Gaucher, C., Poulton, S.W., Canfield, D.E., 2009. Fluctuations in Precambrian atmospheric oxygenation recorded by chromium isotopes. *Nature* 461, 250–253.
- Fujimoto, D., Tamiya, N., 1962. Incorporation of ¹⁸O from air into hydroxyproline by chick embryo. *Biochem. J.* 84, 333–335.
- Gingras, M., Hagadorn, J.W., Seilacher, A., Lalonde, S.V., Pecoits, E., Petrash, D., Konhauser, K.O., 2011. Possible evolution of mobile animals in association with microbial mats. *Nat. Geosci.* 4, 372–375.
- Gnaiger, E., Mendez, G., Hand, S.C., 2000. High phosphorylation efficiency and depression of uncoupled respiration in mitochondria under hypoxia. *Proc. Natl. Acad. Sci. USA* 97, 11080–11085.
- Gooday, A.J., Bett, B.J., Escobar, E., Ingole, B., Levin, L.A., Neira, C., Raman, A.V., Sellanes, J., 2010. Habitat heterogeneity and its influence on benthic biodiversity in oxygen minimum zones. *Mar. Ecol. Prog. Ser.* 401, 125–147.
- Gooday, A.J., Levin, L.A., da Silva, A.A., Bett, B.J., Cowie, G.L., Dissard, D., Gage, J.D., Hughes, D.J., Jeffreys, R., Lamont, P.A., Larkin, K.E., Murty, S.J., Schumacher, S., Whitcraft, C., Wouds, C., 2009. Faunal responses to oxygen gradients on the Pakistan margin: a comparison of foraminiferans, macrofauna and megafauna. *Deep-Sea Res.* 56, 488–502.
- Gromet, L.P., Dymek, R.F., Haskin, L.A., Korotev, R.L., 1984. The "North American shale composite": its compilation, major and trace element characteristics. *Geochim. Cosmochim. Acta* 48, 2469–2482.
- Hofmann, A., Peltzer, E., Walz, P., Brewer, P., 2011. Hypoxia by degrees: establishing definitions for a changing ocean. *Deep Sea Res. Pt. I: Oceanogr. Res. Pap.* 58, 1212–1226.
- Holland, H.D., Beukes, N.J., 1990. A paleoweathering profile from Griqualand West, South Africa: evidence for a dramatic rise in atmospheric oxygen between 2.2 and 1.9 bybp. *Am. J. Sci.* 290A, 1–34.
- Ingole, B.S., Sautya, S., Sivadras, S., Singh, R., Nanajkar, M., 2010. Macrofaunal community structure in the western Indian continental margin including the oxygen minimum zone. *Mar. Ecol. Prog. Ser.* 401, 148–166.
- Jeffreys, R.M., Levin, L.A., Lamont, P.A., Wouds, C., Whitcraft, C.R., Mendoza, G.F., Wolff, G.A., Cowie, G.L., 2012. Living on the edge: single-species dominance at the Pakistan oxygen minimum zone boundary. *Mar. Ecol. Prog. Ser.* 470, 79–99.
- Johnston, D.T., Poulton, S.W., Dehler, C.M., Porter, S., Canfield, D.E., Knoll, A.H., 2010. An emerging picture of Neoproterozoic ocean chemistry: insights from the Chuar Group, Grand Canyon, USA. *Earth Planet. Sci. Lett.* 290, 64–73.
- Johnston, D.T., Fischer, W.W., 2012. Stable isotope geobiology. In: Knoll, A.H., Canfield, K.O., Konhauser, K.O. (Eds.), *Fundamentals of Geobiology*. Blackwells, Chichester, pp. 250–266.
- Kah, L.C., Bartley, J.K., 2011. Protracted oxygenation of the Proterozoic biosphere. *Int. Geol. Rev.* 53, 1424–1442.
- Karlstrom, K.E., Bowring, S.A., Dehler, C.M., Knoll, A.H., Porter, S.M., Des Marais, D.J., Weil, A.B., Sharp, Z.D., Geissman, J.W., Elrick, M.B., 2000. Chuar Group of the Grand Canyon: record of breakup of Rodinia, associated change in the global carbon cycle, and ecosystem expansion by 740 Ma. *Geology* 28, 619–622.
- King, N., Westbrook, M.J., Young, S.L., Kuo, A., Abedin, M., Chapman, J., Fairclough, S., Hellsten, U., Isogai, Y., Letunic, I., Marr, M., Pincus, D., Putnam, N., Rokas, A., Wright, K.J., Zuzow, R., Dirks, W., Good, M., Goodstein, D., Lemons, D., Li, W., Lyons, J.B., Morris, A., Nichols, S., Richter, D.J., Salamov, A., Sequencing, J., Bork, P., Lim, W.A., Manning, G., Miller, W.T., McGinnis, W., Shapiro, H., Tijan, R., Grigoriev, I.V., Rokhsar, D., 2008. The genome of the choanoflagellate *Monosiga brevicollis* and the origin of metazoans. *Nature* 451, 783–788.
- Knoll, A.H., 2011. The multiple origins of complex multicellularity. *Annu. Rev. Earth Planet. Sci.* 39, 217–239.
- Knoll, A.H., Bambach, R.K., Payne, J.L., Pruss, S., Fischer, W., 2007. Paleophysiology and end-Permian mass extinction. *Earth Planet. Sci. Lett.* 256, 295–313.
- Knoll, A.H., Carroll, S.B., 1999. Early animal evolution: emerging views from comparative biology and geology. *Science* 284, 2129–2137.
- Knoll, A.H., Javaux, E.J., Hewitt, D., Cohen, P., 2006. Eukaryotic organisms in Proterozoic oceans. *Philos. Trans. R. Soc. London Ser. B* 361, 1023–1038.
- Kodner, R.B., Summons, R.E., Pearson, A., King, N., Knoll, A.H., 2008. Sterols in a unicellular relative of the metazoans. *Proc. Natl. Acad. Sci. USA* 105, 9897–9902.
- Kump, L.R., 2008. The rise of atmospheric oxygen. *Nature* 451, 277–278.
- Kump, L.R., Pavlov, A., Arthur, M.A., 2005. Massive release of hydrogen sulfide to the surface ocean and atmosphere during intervals of oceanic anoxia. *Geology* 33, 397–400.
- Lamont, P.A., Gage, J.D., 2000. Morphological responses of macrobenthic polychaetes to low oxygen on the Oman continental slope, NW Arabian Sea. *Deep-Sea Res.* 47, 9–24.
- Lartillot, N., Lepage, T., Blanquart, S., 2009. PhyloBayes 3: a Bayesian software package for phylogenetic reconstruction and molecular dating. *Bioinformatics* 25, 2286–2288.
- Levin, L., Ekau, W., Gooday, A., Jorissen, F., Middelburg, J., Naqvi, W., Neira, C., Rabalais, N., Zhang, J., 2009. Effects of natural and human-induced hypoxia on coastal benthos. *Biogeosci. Discuss.* 6, 3563–3654.
- Levin, L., Gutierrez, D., Rathburn, A., Neira, C., Sellanes, J., Munoz, P., Gallardo, V., Salamanca, M., 2002. Benthic processes on the Peru margin: a transect across the oxygen minimum zone during the 1997–98 El Niño. *Prog. Oceanogr.* 53, 1–27.
- Levin, L.A., 2003. Oxygen Minimum Zone benthos: adaptation and community response to hypoxia. *Oceanogr. Mar. Biol.: Annu. Rev.* 41, 1–45.
- Levin, L.A., Huggett, C.L., Wishner, K.F., 1991. Control of deep-sea benthic community structure by oxygen and organic-matter gradients in the eastern Pacific Ocean. *J. Mar. Res.* 49, 763–800.
- Love, G.D., Grosjean, E., Stalvies, C., Fike, D.A., Grotzinger, J.P., Bradley, A.S., Kelly, A.E., Bhatia, M., Meredith, W., Snape, C.E., Bowring, S.A., Condon, D.J., Summons, R.E., 2009. Fossil steroids record the appearance of Demospongiae during the Cryogenian period. *Nature* 457, 718–721.
- Lyons, T.W., Severmann, S., 2006. A critical look at iron paleoredox proxies: new insights from modern euxinic marine basins. *Geochim. Cosmochim. Acta* 70, 5698–5722.
- Macdonald, F.A., Halverson, G.P., Strauss, J.V., Smith, E.F., Cox, G., Sperling, E.A., Roots, C.F., 2012. Early Neoproterozoic basin formation in the Yukon: implications for the make-up and break-up of Rodinia. *Geosci. Can.* 39, 77–99.
- Macdonald, F.A., Schmitz, M.D., Crowley, J.L., Roots, C.F., Jones, D.S., Maloof, A.C., Strauss, J.V., Cohen, P.A., Johnston, D.T., Schrag, D.P., 2010. Calibrating the Cryogenian. *Science* 327, 1241–1243.
- Nagy, R.M., Porter, S.M., Dehler, C.M., Shen, Y., 2009. Biotic turnover driven by eutrophication before the Sturtian low-latitude glaciation. *Nat. Geosci.* 2, 415–418.
- Narbonne, G.M., 2011. When life got big. *Nature* 470, 339–340.
- Neira, C., Gad, G., Arroyo, N.L., Decraemer, W., 2001. *Glochinema bathyperuvensis* sp. n. (Nematoda, Epsilonematidae): a new species from Peruvian bathyal sediments, SE Pacific Ocean. *Contrib. Zool.* 70, 147–159.
- Nesbitt, H., Young, G., 1982. Early Proterozoic climates and plate motions inferred from major element chemistry of lites. *Nature* 299, 715–717.
- Och, L.M., Shields-Zhou, G.A., 2012. The Neoproterozoic oxygenation event: environmental perturbations and biogeochemical cycling. *Earth Sci. Rev.* 110, 26–57.
- Palma, M., Quiroga, E., Gallardo, V.A., Arntz, W., Gerdes, D., Schneider, W., Hebbeln, D., 2005. Macrobenthic animal assemblages of the continental margin off Chile (22° to 42° S). *J. Mar. Biol. Assoc. UK* 85, 233–245.
- Parfrey, L.W., Lahr, D.J.G., Knoll, A.H., Katz, L.A., 2011. Estimating the timing of early eukaryotic diversification with multigene molecular clocks. *Proc. Natl. Acad. Sci. USA* 108, 13624–13629.
- Paulmier, A., Ruiz-Pino, D., Garçon, V., Farias, L., 2006. Maintaining of the eastern south Pacific oxygen minimum zone (OMZ) off Chile. *Geophys. Res. Lett.* 33, L20601.
- Pavlov, A., Kasting, J., 2002. Mass-independent fractionation of sulfur isotopes in Archean sediments: strong evidence for an anoxic Archean atmosphere. *Astrobiology* 2, 27–41.
- Payne, J.L., McClain, C.R., Boyer, A.G., Brown, J.H., Finnegan, S., Kowalewski, M., Krause, J.R.A., Lyons, S.K., McShea, D.V., Novack-Gottshall, P.M., Smith, F.A., Spaeth, P., Stempien, J.A., Wang, S.C., 2010. The evolutionary consequences of oxygenic photosynthesis: a body size perspective. *Photosynth. Res.* 107, 37–57.
- Peters, S.E., Loss, D.P., 2012. Storm and fair-weather wave base: a relevant distinction? *Geology* 40, 511–514.
- Philippe, H., Brinkmann, H., Lavrov, D.V., Littlewood, D.T.J., Manuel, M., Worheide, G., Baurain, D., 2011. Resolving difficult phylogenetic questions: why more sequences are not enough. *PLoS Biol.* 9, e1000602.
- Philippe, H., Derelle, R., Lopez, P., Pick, K., Borchellini, C., Boury-Esnault, N., Vacelet, J., Deniel, E., Houlston, E., Queinnee, E., Da Silva, C., Wincker, P., Le Guyader, H., Lays, S., Jackson, D.J., Scheiber, F., Erpenbeck, D., Morgenstern, B., Worheide, G., Manuel, M., 2009. Phylogenomics restores traditional views on deep animal relationships. *Curr. Biol.* 19, 706–712.
- Planavsky, N.J., Rouxel, O.J., Bekker, A., Lalonde, S.V., Konhauser, K.O., Reinhard, C.T., Lyons, T.W., 2010. The evolution of the marine phosphate reservoir. *Nature* 467, 1088–1090.
- Porter, S.M., Knoll, A.H., 2000. Testate amoeba in the Neoproterozoic Era: evidence from vase-shaped microfossils in the Chuar Group, Grand Canyon. *Paleobiology* 26, 360–385.
- Porter, S.M., Meisterfeld, R., Knoll, A.H., 2003. Vase-shaped microfossils from the Neoproterozoic Chuar Group, Grand Canyon: a classification guided by modern testate amoebae. *J. Paleontol.* 77, 205–225.

- Poulton, S., Raiswell, R., 2002. The low-temperature geochemical cycle of iron: from continental fluxes to marine sediment deposition. *Am. J. Sci.* 302, 774–805.
- Poulton, S.W., Canfield, D.E., 2005. Development of a sequential extraction procedure for iron: implications for iron partitioning in continentally derived particulates. *Chem. Geol.* 214, 209–221.
- Poulton, S.W., Canfield, D.E., 2011. Ferruginous conditions: a dominant feature of the ocean through Earth's history. *Elements* 7, 107–112.
- Prockop, D., Kaplan, A., Udenfriend, S., 1963. Oxygen-18 studies on the conversion of proline to collagen hydroxyproline. *Arch. Biochem. Biophys.* 101, 499–503.
- Raff, R.A., Raff, E.C., 1970. Respiratory mechanisms and the metazoan fossil record. *Nature* 228, 1003–1005.
- Rainbird, R.H., Jefferson, C.W., Young, G.M., 1996. The early Neoproterozoic sedimentary Succession B of northwestern Laurentia: correlations and paleogeographic significance. *Geol. Soc. Am. Bull.* 108, 454–470.
- Raiswell, R., Canfield, D.E., 1998. Sources of iron for pyrite formation in marine sediments. *Am. J. Sci.* 298, 219–245.
- Rhoads, D.C., Morse, J.W., 1971. Evolutionary and ecologic significance of oxygen-deficient marine basins. *Lethaia* 4, 413–428.
- Runnegar, B., 1982a. The Cambrian explosion: animals or fossils? *J. Geol. Assoc. Aust.* 29, 395–411.
- Runnegar, B., 1982b. Oxygen requirements, biology and phylogenetic significance of the late Precambrian worm *Dickinsonia*, and the evolution of the burrowing habit. *Alcheringa* 6, 223–239.
- Runnegar, B., 1991. Precambrian oxygen levels estimated from the biochemistry and physiology of early eukaryotes. *Palaeogeogr. Palaeoclimatol. Palaeoecol.* 97, 97–111.
- Ruppert, E.E., Fox, R.S., Barnes, R.D., 2004. *Invertebrate Zoology*. Thomson, Belmont, CA, pp. 1–963.
- Sahoo, S.K., Planavsky, N.J., Kendall, B., Wang, X., Shi, X., Scott, C., Anbar, A.D., Lyons, T.W., Jiang, G., 2012. Ocean oxygenation in the wake of the Marinoan glaciation. *Nature* 489, 546–549.
- Scott, C., Lyons, T.W., Bekker, A., Shen, Y., Poulton, S.W., Chu, X., Anbar, A.D., 2008. Tracing the stepwise oxygenation of the Proterozoic ocean. *Nature* 452, 456–459.
- Shen, Y., Knoll, A.H., Walter, M.R., 2003. Evidence for low sulphate and anoxia in a mid-Proterozoic marine basin. *Nature* 423, 632–635.
- Sperling, E.A., Peterson, K.J., Pisani, D., 2009. Phylogenetic-signal dissection of nuclear housekeeping genes supports the paraphyly of sponges and the monophyly of Eumetazoa. *Mol. Biol. Evol.* 26, 2261–2274.
- Sperling, E.A., Robinson, J.M., Pisani, D., Peterson, K.J., 2010. Where's the glass? Biomarkers, molecular clocks, and microRNAs suggest a 200-Myr missing Precambrian fossil record of siliceous sponges. *Geobiology* 8, 24–36.
- Terwilliger, N.B., 1998. Functional adaptations of oxygen-transport proteins. *J. Exp. Biol.* 201, 1085–1098.
- Thorkelson, D.J., Abbott, J.G., Mortensen, J.K., Creaser, R.A., Velleneuve, M.E., McNicoll, V.J., Laver, P.W., 2005. Early and Middle Proterozoic evolution of Yukon, Canada. *Can. J. Earth Sci.* 42, 1045–1071.
- Tribouillard, N., Algeo, T.J., Lyons, T., Riboulleau, A., 2006. Trace metals as paleoredox and paleoproductivity proxies: an update. *Chem. Geol.* 232, 12–32.
- Towe, K.M., 1970. Oxygen-collagen priority and the early metazoan fossil record. *Proc. Natl. Acad. Sci. USA* 65, 781–788.
- Tyson, R.V., Pearson, T.H., 1991. Modern and ancient continental shelf anoxia: an overview. In: Tyson, R.V., Pearson, T.H. (Eds.), *Modern and Ancient Continental Shelf Anoxia*. Geological Society Special Publications, London, pp. 1–24.
- Vaquier-Sunyer, R., Duarte, C.M., 2008. Thresholds of hypoxia for marine biodiversity. *Proc. Natl. Acad. Sci. USA* 105, 15452–15457.
- Wang, C., Leger, R.J.S., 2006. A collagenous protective coat enables *Metarhizium anisopliae* to evade insect immune responses. *Proc. Natl. Acad. Sci. USA* 103, 6647–6652.
- Zettler, M.L., Bocher, R., Pollehne, F., 2009. Macrozoobenthos diversity in an oxygen minimum zone off northern Namibia. *Mar. Biol.* 156, 1949–1961.